Nanoplastics adsorption and removal efficiency by granular activated carbon used in drinking water treatment process

Ramirez Arenas, Lina Marcela; Ramseier Gentile, Stéphan; Zimmermann, Stéphane; Stoll, Serge

How to cite

RAMIREZ ARENAS, Lina Marcela et al. Nanoplastics adsorption and removal efficiency by granular activated carbon used in drinking water treatment process. In: Science of the Total Environment, 2021, vol. 791, n° 148175. doi: 10.1016/j.scitotenv.2021.148175

This publication URL: https://archive-ouverte.unige.ch/unige:152390
Publication DOI: 10.1016/j.scitotenv.2021.148175

Science of the Total Environment 791 (2021) 148175

Contents lists available at ScienceDirect

Science of the Total Environment

journal homepage: www.elsevier.com/locate/scitotenv

Nanoplastics adsorption and removal efficiency by granular activated carbon used in drinking water treatment process

Lina Ramirez Arenas [a,*], Stéphan Ramseier Gentile [b], Stéphane Zimmermann [b], Serge Stoll [a,*]

[a] Group of Environmental Physical Chemistry, Department F.-A. Forel for Environmental and Aquatic Sciences, University of Geneva, Uni Carl Vogt, 66, boulevard Carl-Vogt, CH-1211 Geneva 4, Switzerland
[b] SIG, Industrial Boards of Geneva, Ch. du Château-Bloch, Le Lignon, 1211 Genève 2, Switzerland

HIGHLIGHTS

- GAC removal efficiency is higher in Lake Geneva water compared to ultrapure water.
- Nanoplastic adsorption capacity is found equal to 6.33 mg/g in Geneva Lake water.
- Nanoplastics and GAC surface charges control removal efficiency.
- DOM and divalent cations play roles on nanoplastics adsorption mechanisms.

GRAPHICAL ABSTRACT

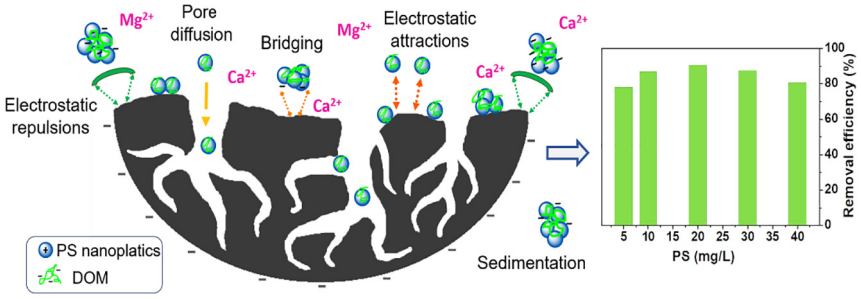

ARTICLE INFO

Article history:
Received 1 April 2021
Received in revised form 26 May 2021
Accepted 26 May 2021
Available online 1 June 2021

Editor: Damia Barcelo

Keywords:
Nanoplastics
Granular Activated Carbon
Adsorption mechanisms
Removal efficiency
Drinking water

ABSTRACT

In this study Granular Activated Carbon (GAC) used in drinking water treatment processes is evaluated for its capacity to adsorb and remove polystyrene (PS) nanoplastics. Batch experiments are conducted in ultrapure and surface water from Lake Geneva, currently used as drinking water resources. Equilibrium and kinetic studies are conducted to understand adsorption mechanisms and limiting factors. Our results show that in ultrapure water the adsorption and removal of PS nanoplastics are mainly due to electrostatic interactions between the positively charged nanoplastics and negatively charged GAC. It is found that the adsorption capacity increases with nanoplastic concentration with a maximum adsorption capacity of 2.20 mg/g. The adsorption kinetics follows a pseudo-second-order model and indicates that the intra-particle diffusion is not the only rate-controlling step. The Langmuir isotherm indicates that nanoplastics are adsorbed as a homogeneous monolayer onto the GAC surface with a maximum monolayer adsorption capacity of 2.15 mg/g in agreement with the experimental value. In Lake Geneva water the adsorption capacity and removal efficiency of PS nanoplastics are found three times higher than in ultrapure water and increase significantly with increasing PS nanoplastics concentration with a maximum adsorption capacity of 6.33 mg/g. This improvement in adsorption capacity is due to the presence of Dissolved Organic Matter (DOM), resulting in PS surface charge modification, presence of divalent ions making possible the adsorption of PS-DOM complexes, and, aggregation of PS nanoplastics. The kinetic pseudo-second-order and intra-particle diffusion provide a good correlation with the experimental data. In contrast, neither Langmuir nor Freundlich isotherms describe in a satisfactory way the adsorption of nanoplastics by GAC. This study reveals that GAC produced from renewable sources can be considered as a moderate adsorbent for the removal of PS nanoplastics in water treatment plants and that the presence of DOM and cationic species play a major role.

* Corresponding authors.
E-mail addresses: Lina.RamirezArenas@unige.ch (L. Ramirez Arenas), Serge.Stoll@unige.ch (S. Stoll).

https://doi.org/10.1016/j.scitotenv.2021.148175

1. Introduction

With increasing productions and applications of plastic materials in every-day life, large amounts of them have been released and accumulated in the environment. Once in the environment plastics can breakdown into smaller particles commonly termed as microplastics and nanoplastics (Alimi et al., 2018; Eerkes-Medrano et al., 2015). Microplastics are defined as plastic particles within a size range from 1 μm to 5 mm (Enfrin et al., 2019; Sobhani et al., 2020), while plastic particles between 1 and 1000 nm are categorized as nanoplastics (Zhang et al., 2021; Zhang et al., 2020a). Micro and nanoplastics can be categorized in two different types, primary and secondary micro and nanoplastics. Primary microplastics and nanoplastics are originally manufactured in the micro and nano size range, generally used as abrasive agents and as exfoliants in personal care products (Hernandez et al., 2017; Murphy et al., 2016; Rochman et al., 2015). On the other hand, secondary microplastics and nanoplastics are the result of fragmentation and degradation processes from larger plastic debris (Gigault et al., 2016; Lambert and Wagner, 2016; Tian et al., 2019).

Once released in aquatic systems through wastewater treatment effluents and urban runoff (Besseling et al., 2017; Bhatt and Tripathi, 2011; Park et al., 2017), micro and nanoplastics can reach water compartments used for drinking water production, resulting in a potential consumption of nanoplastics by human (Shams et al., 2020; Zhang et al., 2020b). Microplastics such as polyethylene (PE), polypropylene (PP), polystyrene (PS), polyvinylchloride (PVC), and others types of microplastics have been detected in raw water and drinking water (Mintenig et al., 2019; Novotna et al., 2019; Pivokonsky et al., 2018; Wang et al., 2018). Results may vary significantly from less than 10 microplastic particles/L up to 4000 particles/L and strongly depend on the sampling locations.

Studies mainly focused on drinking water contamination by microplastics, and less attention was given to nanoplastics. It should be noted that the environmental impact of nanoplastics is expected to differ from microplastics. Owing to their high surface area ratio, nanoplastic particles have strong adsorption affinities for contaminants such as heavy metals and persistent organic pollutants (Liu et al., 2018; Mattsson et al., 2015; Wu et al., 2019) but also can accumulate in organisms and reach tissues and organs due to their reduced sizes causing toxicological effects (Baalousha et al., 2010; Saleh, 2020; Zhang et al., 2021).

Similar to engineered nanoparticles (NPs) such as metallic nanoparticles, nanoplastics will undergo a variety of transformation in aquatic systems that will influence their ultimate fate. Natural waters have specific ionic compositions, contain Natural Organic Matter (NOM), and inorganic colloids (IC) that will affect the surface properties and stability of nanoplastics via the formation of heteroaggregates made of nanoplastics, IC and NOM, which will play an important role in their transport process, fate and environmental impact (Labille et al., 2015; Praetorius et al., 2020; Ramirez et al., 2019). Oriekhova and Stoll (2018) investigated the effect of inorganic colloids and NOM on the behavior and stability of positively charged polystyrene (PS) nanoplastics. The authors showed that polystyrene nanoplastics form heteroaggregates with Fe_2O_3 and NOM. They also found that Fe_2O_3, and NOM concentration are important parameters controlling heteroaggregation. Shams et al. (2020) and Dong et al. (2021) showed that divalent ions such as (Ca^{2+} and Mg^{2+}) have a significant effect on the destabilization of the negatively charged polystyrene and polyethylene nanoplastics whereas NOM increases their stability. Shams et al. (2020) concluded that polystyrene nanoplastics are more difficult to destabilize compared to polyethylene nanoplastics which can aggregate easily at low ionic strength. Those results indicate that nanoplastics properties and more specifically surface charge properties will play an important role on their environmental impact.

In addition to natural waters, it is also important to evaluate how nanoplastic particles can be effectively removed through water treatment processes, to control and limit environmental and health risks associated with nanoplastics exposure. In particular, processes such as sand filtration and granulated or powdered activated carbon filtration are widely used in drinking water treatment plants to remove a variety of pollutants from water because of their high efficiency, technical simplicity, and environmental friendly and safe materials (Mutemi et al., 2020; Piai et al., 2020; Xu et al., 2016). Several studies have reported that engineered nanoparticles can be removed from water by adsorption process (Chowdhury et al., 2011; Degenkolb et al., 2018; Inyang et al., 2013; Kamrani et al., 2018; Li et al., 2013; Rottman et al., 2013). These studies reported that removal of NPs was controlled by adsorbent material, NPs and water physicochemical properties. With regards to nanoplastics removal, Tong et al. (2020) investigated the removal of 20 nm and 200 nm polystyrene nanoplastics by sand filtration. Their results indicated an increase of nanoplastics retention with increasing the medium ionic strength. According to the authors, nanoplastics retention was further increased (from 22% to 98% approx.) with the introduction of Fe_3O_4-biochar to the sand column. In another study, Zhang et al. (2020c) investigated the removal efficiency of 180 nm polystyrene nanoplastics by anthracite filtration. The authors found that 98.9% ± 0.7 of nanoplastics were removed from raw water by filtration process, whereas the coagulation/flocculation and sedimentation process were less effective on removing nanoplastics. Murray and Örmeci (2020) also investigated the efficiency of filtration to remove nanoplastics <400 nm using different filter pore sizes and materials from 0.02 to 3 μm. Their results showed that 92% ± 3 of nanoplastics were removed from tap water with 0.02 μm filter pore.

Activated carbons are the most used adsorbent material in drinking water treatment process due to their high surface area, porous structure and have shown to be very efficient for the removal of organic and inorganic pollutants from drinking water and wastewaters (Foo and Hameed, 2009; Largitte and Pasquier, 2016; Okonji et al., 2021; Xu et al., 2016). A previous study investigated the ability of activated carbon to remove ZnO and CuO NPs from deionized water and wastewater (Piplai et al., 2017). In their study, Piplai et al. found that the removal of ZnO and CuO NPs in wastewater by activated carbon was less effective than in deionized water due to the wastewater compounds, which resulted in a reduction of adsorption active sites by fouling or clogging. The authors concluded that NPs are removed from water by sedimentation, electrostatic attractions and surface complexation. McGillicuddy et al. (2018) investigated the ability of milled activated carbon to remove Ag NPs from deionized and fresh water samples. The authors found that the removal of Ag NPs increased with decreasing concentration and increasing contact time with the activated carbon. They concluded that milled activated carbon, can successfully capture Ag NPs from water samples. To our knowledge, studies concerning the adsorption and removal of nanoplastics on granular activated carbon have not been reported yet.

Release and accumulation of nanoplastics in aquatic systems and consequently water compartments used for drinking water production represent a global concern in terms of environmental impact and potential risks to human health. Therefore, owing to the importance of adsorption processes based on activated carbon in drinking water plants and needs in the understanding of adsorption mechanisms and evaluation of nanoplastic removal, the objective of the present work is to evaluate the adsorption efficiency of granular coconut shell-based activated carbon for the removal of amidine polystyrene (PS) nanoplastics with diameter of 100 nm, get an insight into the adsorption mechanisms, and isolate important parameters. Furthermore, we are convinced that there are many drinking water suppliers who are questioning both the effectiveness of their existing treatment processes in removing nanoplastics from surface waters that are being treated, and the optimization of the water treatment processes.

In this study, well-defined and calibrated positively charged PS beads are used as a surrogate nanoplastic model. Positively charged nanoplastics were selected since they were found to be more toxic to living organisms when compared to negatively charged particles

(Bergami et al., 2017; Saavedra et al., 2019). It should also be noted that the granular compound considered here is largely used in drinking water treatment processes and produced from renewable sources, which represents a sustainable solution for water purification.

2. Materials and methods

Batch experiments are conducted in ultrapure water and natural surface water from Lake Geneva, currently used as the drinking water resource for half a million of consumers, to get an insight on PS nanoplastic behavior, adsorption and removal processes. To quantify the adsorption process, different adsorption models are applied to the experimental data to evaluate the adsorption capacity and removal efficiency of the adsorbent. Moreover, Scanning Electron Microscopy (SEM) image analysis as well as nanoplastic particle surface charge variations and aggregation are considered to better understand PS nanoplastic adsorption, balance between adsorption and aggregation, and derive adsorption mechanisms.

2.1. Materials

Surfactant-free polystyrene latex nanosplastics were obtained as a solution from Thermo Fisher Scientific-1862725 (Rheinach, Switzerland) with a determined manufactured transmission electronic microscopy (TEM) diameter of 90 ± 7 nm, a density equal to 1.055 g/cm^3 at 20 °C and a specific surface area of 63 m^2/g. Stock suspensions of 3 g/L were prepared from the original solution which, contained 40 g/L of PS nanoplastic particles with amidine functional groups on the surface, and diluted with ultrapure water (Milli Q water, Millipore, Switzerland, with $R >$ 18 MΩ·cm, total organic carbon (TOC) < 2 ppb). PS stock suspension was sonicated during 15 min with a sonication bath (Bransonic ultra cleaner, Branson 5510 model, Switzerland) before use. The stock solution was stored in a dark place at constant temperature of 4 °C and used for further experiments.

Granular coconut shell-based Activated Carbon (AquaSorb™ CX) used in this study is a commercial carbon from JACOBI Carbons, used in drinking water treatment and provided by SIG (Industrial Boards of Geneva). The characteristics of the Granular Activated Carbon (GAC) including the specific surface area, mean particle diameter (mm), and hardness are given in Table S1. Prior to its use, GAC was cleaned to remove impurities and residual ions adsorbed on its surface. The cleaning protocol of GAC is described in the supplementary information (S1).

Lake Geneva water was taken at the inlet of the drinking water treatment plant in Geneva. The physicochemical properties of Lake Geneva water including pH, conductivity, water hardness, and Dissolved Organic Carbon (DOC) are given in Table S2. pH and conductivity were measured using a Hach Lange HQ40d portable meter (Hach Lange, Switzerland). The major ion composition of Lake Geneva water was determined by chromatographic analysis (ICS 3000, Dionex, Switzerland) and given in Table S3. Dissolved organic carbon concentration was measured using a Shimadzu TOC-L instrument (Shimadzu Scientific Instruments, Japan). Water from Lake Geneva was filtered using a membrane filter with pore size equal to 0.2 μm (Merck Millipore Ltd., Switzerland) before each experiment. The water sample was stored in a dark place at constant temperature of 4 °C.

2.2. Methods

2.2.1. Zeta potential and size distribution measurements

ζ (zeta)-Potential and z-average hydrodynamic diameter of PS nanoplastics in ultrapure and Lake Geneva waters were determined by electrophoretic mobility and dynamic light scattering (DLS) methods respectively, using a Zetasizer Nano ZS (Malvern Instruments Ltd.; Malvern, UK). The Smoluchowski equation was applied to calculate the ζ-potential values from the electrophoretic mobility (Baalousha, 2009; Lowry et al., 2016; Ortelli et al., 2017). Each ζ-potential and z-average hydrodynamic diameter value was measured from two experimental replicates with five parallel measurements of fifteen runs with a delay of 5 s between them to stabilize the system.

2.2.2. Turbidity measurements

GAC adsorption capacity and nanoplastics removal efficiency is based in this study on turbidity (nephelometric) measurements. Several challenges need to be overcome when quantifying nanoplastics in complex matrices such as the tedious and time-consuming extraction before quantification. Such limitations make real-time quantification of nanoplastics for example at a full-scale water treatment plant extremely challenging and turbidity measurements constitute a good option in such a context. For example, turbidity was used by Murray and Örmeci (2020) to evaluate the nanoplastics removal after coagulation and filtration treatment and authors concluded that turbidity is an effective and rapid technique for measuring nanoplastic concentrations. In addition, turbidity measurements are generally used in drinking water treatment plants as a regulator parameter of particulate contamination in water and play an important part in water quality monitoring (Gregory, 1998) and these last years instrument development and sensitivity has advanced significantly.

Turbidity of PS nanoplastic suspensions was measured in our experiments using a Hach Turbidimeter TU5200 with an infra-red emitting laser at 850 nm (Hach Lange, Switzerland). The light scattered at an angle of 90° from the incident light is measured at 360° using multiple detectors located around the sample cell. This provides high accuracy at low turbidity ranges and better reproducibility.

Calibration curves for PS nanoplastics in ultrapure and Lake Geneva waters was established by plotting turbidity versus known PS nanoplastic concentrations. Each value represents the mean of two experimental replicates with two parallel measurements. As shown in Fig. S1, good correlation coefficients ($R^2 = 0.99$) were obtained for both ultrapure water and Lake Geneva water, indicating that turbidity measurements in our case is a sensitive and accurate technique that can be used as an indicator of nanoplastics removal efficiency.

The concentration of PS nanoplastics before and after batch adsorption experiments was determined measuring the turbidity of the supernatant suspension at different time intervals. Prior to analysis, the instrument was calibrated with StablCal solutions from Hach, and the light scattered by the particles was measured in Formazine Nephelometric Unit (FNU).

2.2.3. Scanning Electron Microscope (SEM)

Scanning Electron Microscope analysis of PS nanoplastics and GAC samples were performed in ultrapure and Lake Geneva water, before and after PS adsorption experiments. JSM-7001FA scanning electron microscope (JEOL, Japan) was used to get an insight into the GAC surface and pore properties, PS nanoplastic morphology, adsorption, surface distribution and aggregation state. SEM images of PS nanoplastics were obtained dropping 10 μL of PS sample on one aluminum stub covered with 5 × 5 mm silica wafer (Agar Scientific G3390) and coated with 5 nm layer of gold. GAC samples were placed on a conductive carbon tape and wrapped with 5 nm gold coating.

2.3. Experimental procedure

2.3.1. PS nanoplastics and activated carbon characterization

To characterize PS nanoplastics and activated carbon surface charge in different pH conditions, pH titration curves were performed in ultrapure water for pH values in a range of 2 to 11. PS nanoplastic suspension of 20 mg/L was prepared at pH 3.1 ± 0.1 by adding the appropriate amount of PS from the stock suspension, then the pH was increased. Measurements of ζ-potential and z-average hydrodynamic diameters were performed 10 min after pH modification to ensure pH stabilization. Activated carbon suspension of 5 g/L was prepared in ultrapure water at pH 2.0 ± 0.1 by adding powdered activated carbon previously pulverized with an agate pestle and mortar, then the pH was increased

to 11 ± 0.1. ζ-potential measurements were performed 10 min after pH modification. Diluted hydrochloric acid and sodium hydroxide (HCl and NaOH, Titrisol® 113, Merck, Switzerland) were used to adjust the suspension pH.

2.3.2. Batch adsorption experiments

Batch adsorption experiments were performed in 150 mL polypropylene plastic flasks containing 30 mL of PS nanoplastics suspension with initial concentrations from 5 to 40 mg/L. Variable amounts of GAC were used and added to each flask before the addition of PS suspension. Suspensions were shaken on an orbital shaker at 100 rpm for a contact time of 240 min at room temperature. The flask was removed from the shaker and the concentration, ζ-potential, and z-average hydrodynamic of PS nanoplastics in the supernatant were measured. Prior to analysis, all samples were left to settle down for 30 min in other to minimize interference of carbon particles with the analysis. The sedimentation time of 30 min was determined experimentally. PS nanoplastic-free control suspensions (with GAC and without nanoplastics) were also carried out to evaluate the carbon particles interference with turbidity measurements (Fig. S1c and d). These data were used to calculate the PS nanoplastics concentration in the supernatant suspension.

Experiments were first performed in ultrapure water at pH 7.4 ± 0.1, in the pH range of natural waters, and corresponding to a domain where PS nanoplastics are stable regarding aggregation and exhibit highly positive surface charges as shown in Fig. 1a. Then, experiments were conducted in Lake Geneva water at its natural pH (8.4 ± 0.1) to get an insight into the effect of environmental conditions on PS nanoplastics behavior and adsorption process. For each experiment, duplicates and adsorbent-free control suspensions were performed in parallel under identical conditions to evaluate nanoplastics stability in solution (Figs. S2 and S3).

2.3.3. Effect of adsorbent concentration

In order to evaluate the effect of adsorbent concentration on the adsorption of PS nanoplastics and determine the GAC optimal concentration for subsequent studies. Experiments were first carried out in ultrapure water at adsorbent concentrations from 3 to 15 g/L and fixed PS nanoplastic concentration (30 mg/L). The concentration of PS in the supernatant after different time intervals was determined by turbidity measurements. The amount of PS nanoplastics adsorbed per gram of GAC as a function of time, q_t (mg/g) was calculated according to the following equation,

$$q_t = \frac{(C_i - C_f)}{m} V \quad (1)$$

where C_i and C_f (mg/L) are the initial and final concentration of PS nanoplastics in the supernatant at time t (min). V (L) is the volume of the solution and m (g) is the mass of GAC used. The nanoplastic particle removal efficiency (R) was calculated according to the following equation,

$$R = \frac{(C_i - C_f)}{C_i} 100\% \quad (2)$$

where C_f (mg/L) corresponds to the final concentration of PS nanoplastics after 240 min of contact time.

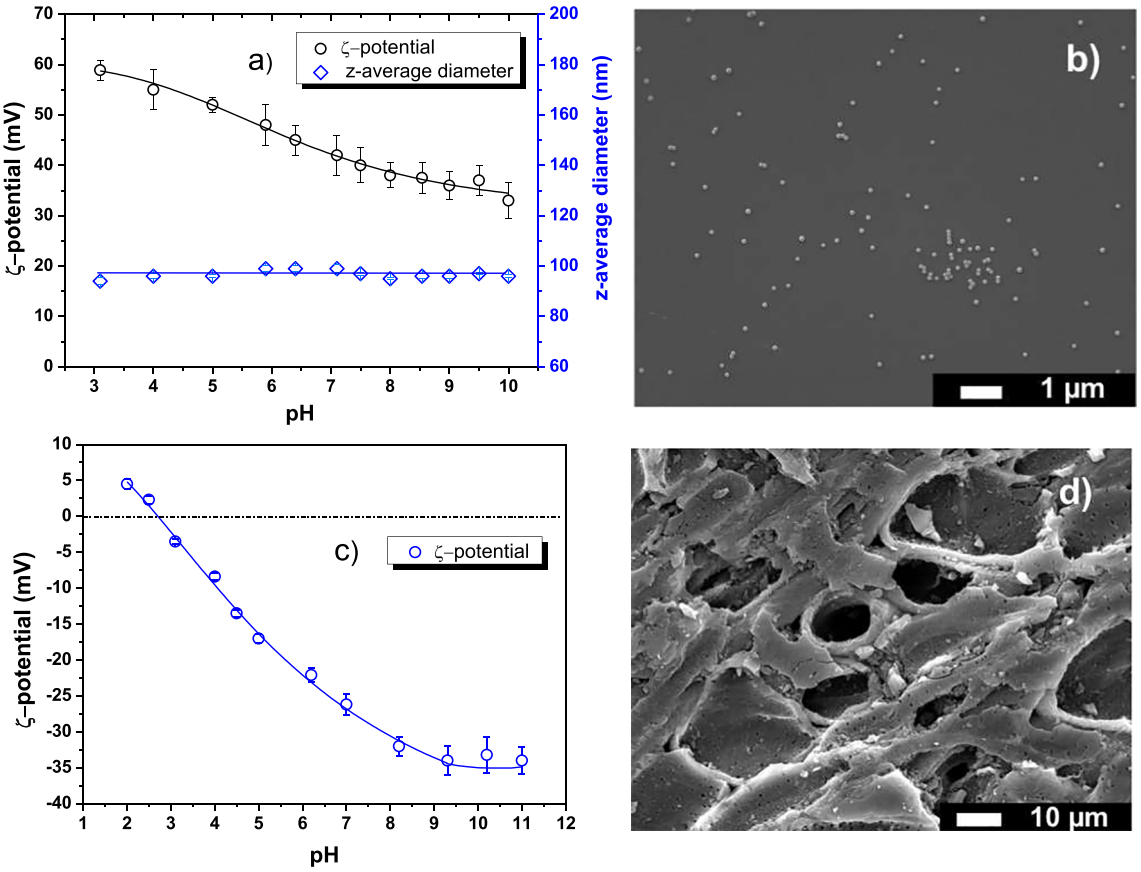

Fig. 1. (a) ζ-Potential and z-average hydrodynamic diameter variation of PS nanoplastics (20 mg/L) as a function of pH in ultrapure water. PS nanoplastics are found highly positively charged and stable within the whole pH range. (b) SEM image of nanoplastic particles (1 mg/L) in ultrapure water at pH 7.4 ± 0.1. Nanoplastic particles are found spherical and dispersed. (c) ζ-Potential of 5 g/L activated carbon in ultrapure water, the point of zero charge (PZC) is found at $pH_{pzc} = 2.7 \pm 0.1$. (d) SEM image of GAC, the surface of GAC is rough with a significant number of pores with sizes between 15 µm and 100 nm, approximatively.

2.3.4. Kinetic and equilibrium studies

Kinetic and equilibrium experiments were conducted in ultrapure and Lake Geneva waters by adding 30 mL of PS nanoplastic solution at different initial concentrations (from 5 to 40 mg/L) into a fixed amount of GAC (5 g/L). The concentration of PS nanoplastics in the supernatant was determined by turbidity at different time intervals as previously described. The amount of PS nanoplastics adsorbed at equilibrium per gram of GAC was calculated according to the following equation.

$$q_e = \frac{(C_i - C_e)}{m} V \quad (3)$$

where C_i represents the PS initial concertation and C_e (mg/L) the concentration of PS nanoplastics at the equilibrium and V (L) the volume of the solution and m (g) the mass of GAC used.

3. Results and discussion

3.1. PS nanoplastics and activated carbon characterization

The surface charge values and stability of PS nanoplastic particles were characterized in ultrapure water by measuring the ζ potential and z-average hydrodynamic diameter variations as a function of pH. As shown in Fig. 1a, PS nanoplastics are found strongly positively charged with ζ-potential equal to +58.9 ± 2.0 mV at pH 3.1 ± 0.1. By increasing further the pH, the surface charge of nanoplastics decreases to +33 ± 3.5 mV at pH 10.0 ± 0.1. PS nanoplastics are highly positively charged and stable within the whole pH range with a mean z-average diameter equal to 97 ± 2 nm due to the positively charged amidine functional groups and resulting electrostatic repulsions. SEM image (Fig. 1b) shows that PS nanoplastics are spherical and dispersed, with an average diameter of 91 ± 9 nm (Fig. S4), which is in agreement with DLS measurements and the size provided by the manufacturer.

Surface charge variation of activated carbon as a function of pH in ultrapure water is given in Fig. 1c. The ζ-potential values indicate that the activated carbon surface charge is mostly negative over the investigated pH range. At pH 2.0 ± 0.1 activated carbon particles are positively charged with ζ-potential values equal to +4.5 ± 0.7 mV, then charge reversal is observed at pH 3.0 ± 0.1 with values equal to −3.5 ± 0.7 mV. The Point of Zero Charge (PZC) is found here at pH 2.7 ± 0.1, similar to the values obtained by Xu et al. (2016). By increasing further the pH, ζ-potential values decrease to −34 ± 2 mV at pH 11.0 ± 0.1.

SEM image in Fig. 1d shows the surface morphology of GAC before adsorption of PS nanoplastics. From the image it can be noted that GAC has a significant number of pores with different sizes and shapes. GAC pores are relatively large with sizes varying between 15 μm and 10 μm approximately, giving an additional surface for PS nanoplastic particles to settle and penetrate. Smaller pores are also found with sizes comprised between 100 nm and 1 μm.

3.2. Batch adsorption studies in ultrapure water

3.2.1. Effect of adsorbent concentration

The effect of adsorbent concentration on PS nanoplastics adsorption was investigated at different GAC doses (from 3 to 15 g/L) and fixed concentration of PS nanoplastics (30 mg/L). As shown in Fig. S5a, the adsorption of PS nanoplastics is rapid in the initial stage then adsorption becomes less efficient especially at high adsorbent concentrations. Results also indicate an increase of the adsorption capacity (mg/g) with decreasing adsorbent concentration, and the maximum PS adsorption is obtained here at 3 g/L of GAC. This increase in PS adsorption with decreasing adsorbent concentration is generally attributed to the availability of adsorption sites. When adsorbent concentration is low, particles can easily access the adsorption sites. On the other hand, PS nanoplastics removal efficiency increases with the adsorbent concentration (Fig. S5b) because of the absolute increasing surface area and number of adsorption sites with GAC doses (Bhattacharyya and Gupta, 2008; Ekmekyapar et al., 2006; Rengaraj et al., 2002). In our case, the removal efficiency of PS nanoplastics increases rapidly up to 38% until the dosage of 7 g/L then increases slowly to 15 g/L GAC corresponding to 50% of removal. All PS nanoplastic suspensions were stable during all experiments and no aggregation and pH modification were observed with the different GAC dosages.

3.2.2. Effect of initial PS nanoplastics concentration and contact time

The effect of initial PS nanoplastics concentration on the adsorption capacity and removal efficiency of GAC is given in Fig. 2. Experiments were carried out at fixed adsorbent concentration (5 g/L) and different initial PS concentrations ranging from 5 to 40 mg/L in ultrapure water at pH 7.4 ± 0.1. A concentration of 5 g/L of GAC was chosen to achieve a good balance between removal efficiency, adsorption capacity and turbidity measurement conditions.

Results show an increase of the adsorption capacity (mg/g) with increasing PS concentration from 5 to 40 mg/L and contact time (Fig. 2a). This can be explained by the PS increasing concentration gradient that provides a greater mass driving force effect, increasing the diffusion of PS nanoplastics from the solution to the GAC. It is also found that PS nanoplastics are rapidly adsorbed at the initial state of the adsorption process, then the adsorption of PS onto GAC becomes less efficient in agreement with the fact that most of the adsorbent sites are available for adsorption during the initial state with gradual occupancy of these adsorption sites until saturation (Ebrahimian Pirbazari et al., 2014; Fu

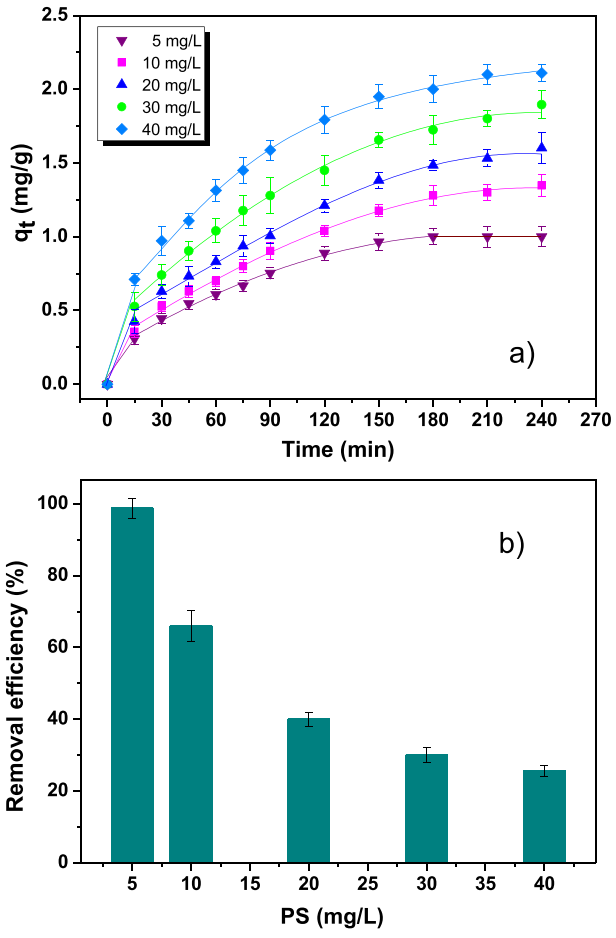

Fig. 2. (a) Effect of initial PS nanoplastics concentration and contact time on the adsorption capacity of 5 g/L GAC in ultrapure water at pH 7.4 ± 0.1 at room temperature and shaker agitation speed of 100 rpm. (b) Effect of initial PS nanoplastics concentration on the removal efficiency at 5 g/L GAC in ultrapure water at pH 7.4 ± 0.1 after 240 min of contact. The maximum removal efficiency (98%) is obtained at 5 mg/L PS nanoplastics.

et al., 2015; Hameed, 2008). As shown in Fig. 2b, increasing PS concentration from 5 to 40 mg/L, results in a decrease in the removal efficiency from 98% to 26%, respectively, after 240 min of contact time. As PS concentration increases, the saturation of GAC active sites increases more rapidly than the PS concentration increase. Therefore, more PS nanoparticles are found in the supernatant with increasing concentration resulting in a decrease of the PS removal efficiency.

3.2.3. Kinetic adsorption rates

To investigate the mechanism of adsorption and rate-controlling steps, the Lagergren pseudo-first-order and pseudo-second-order kinetic models were applied to fit and interpret the experimental data. The pseudo-first-order assumes that the rate-controlling step is a physical process while the pseudo-second-order models rely on a chemical process (Ho and McKay, 1999; Wu et al., 2019), and are expressed respectively as follows:

$$\log\,(\,q_e - q_t\,) = \log\; q_e - \frac{k_1}{2.303}\,t \tag{4}$$

$$\frac{1}{q_t} = \frac{1}{k_2 q_e{}^2} + \frac{t}{q_e} \tag{5}$$

where q_e is the adsorption capacity at equilibrium (mg/g), q_t is the adsorption capacity at time t (mg/g), k_1 is the rate constant of the pseudo-first-order model (1/min) and k_2 is the rate constant of the pseudo-second-order model ((g/mg)/min). The slope and intercept of the plot of log ($q_e - q_t$) versus t (Fig. 3a) are used to determine the rate constant k_1 and the calculated adsorption capacity $q_{e,\mathrm{cal}}$ respectively. The pseudo-second-order rate constant k_2 and the calculated adsorption capacity $q_{e,\mathrm{cal}}$ were calculated from the intercept and slope of the plot of t/q_t versus t (Fig. 3b). Between the two kinetic models, the pseudo-second-order equation shows the best fit to the experimental data, and all the correlation coefficients are greater than 0.98 (Table 1). The values of the rate constant k_2 are found to increase with decreasing PS initial concentration which indicates that the interaction between PS nanoplastics and the GAC is stronger at lower concentrations, resulting in a faster adsorption process. Results suggest the applicability of the pseudo-second-order model which assumes that the rate-controlling step is chemisorption.

In general, adsorption processes can be described by three consecutive steps (Ho et al., 2000; Largitte and Pasquier, 2016). First, the external mass transfer of the adsorbate (PS) from the bulk liquid to the external surface of the adsorbent (GAC), followed by the diffusion in pores of the adsorbent and further adsorption within the adsorbent and onto the external surface. The intra-particle diffusion model proposed by Weber and Morris (1963) was applied to elucidate the diffusion mechanism and expressed as follows:

$$q_t = k_d\, t^{1/2} + C \tag{6}$$

where q_t is the adsorption capacity (mg/g) at time t, k_d ((mg/g)/min$^{1/2}$) is the intra-particle diffusion constant calculated from the slope of the linear plot of q_t versus the square root of contact time ($t^{1/2}$) as shown in Fig. 5c. C (mg/g) is the intercept and give an idea about the boundary layer thickness (Hameed, 2008). As shown in Fig. 3c, the plot of q_t versus $t^{1/2}$ indicates two distinct regions, implying that more than one process is controlling adsorption. The first region of the plot is attributed to external mass transfer process, while the second region is attributed to intra-particle diffusion process. Results suggest that the intra-particle diffusion is not the only rate-controlling step but mass transfer effects and surface saturation effects also control the adsorption. The values of k_{d1} and k_{d2} obtained from the slope of the two linear portions at different initial concentrations indicate the rate of the adsorption. As shown in Table 2, the values of k_{d1} are higher than k_{d2} for all PS initial concentrations, suggesting that PS nanoplastics are transported to the

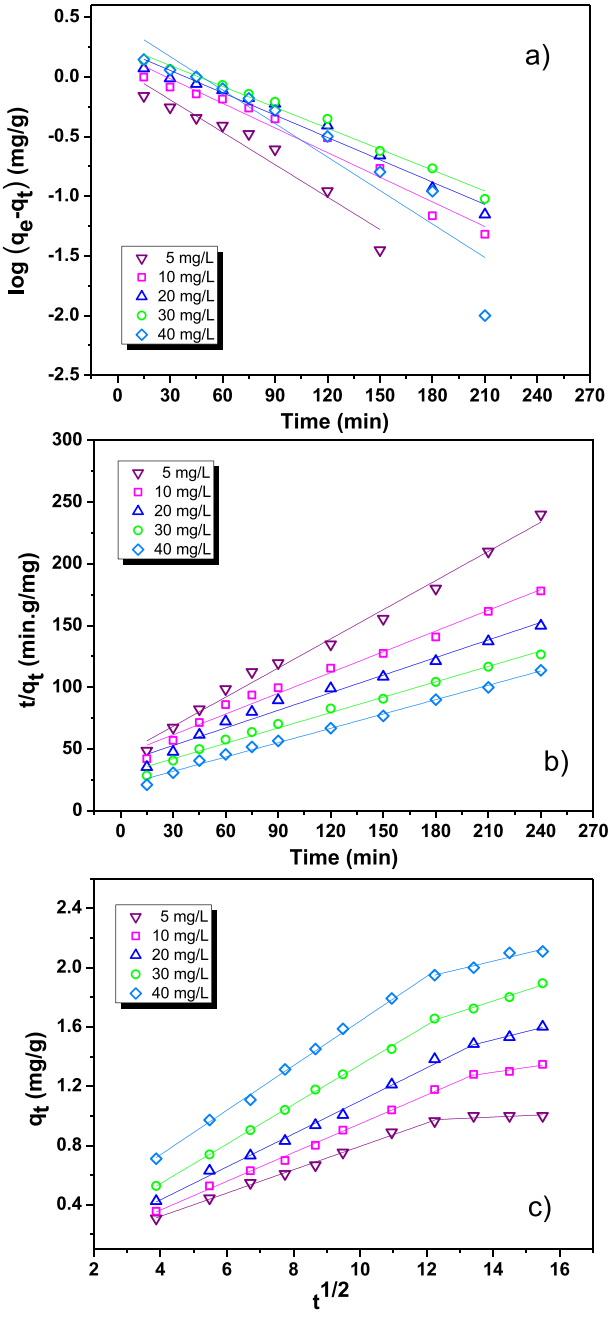

Fig. 3. (a) Pseudo-first order, (b) pseudo-second order and (c) intra-particle diffusion kinetic models for the adsorption of PS nanoplastics at different initial concentrations by 5 g/L GAC in ultrapure water at pH 7.4 ± 0.1. It is found that the pseudo-second-order kinetic models fit better the experimental data ($R^2 > 0.98$).

Table 1
Pseudo-first-order and pseudo-second-order kinetic parameters for the adsorption of PS nanoplastics at different initial concentrations by 5 g/L GAC in ultrapure water at pH 7.4 ± 0.1. Experimental conditions: room temperature, contact time of 240 min and shaker agitation speed of 100 rpm.

C_i (mg/L)	$q_{e\ exp}$ (mg/g)	Pseudo-first-order			Pseudo-second-order		
		$K_1 \times 10^{-2}$ (1/min)	$q_{e\ calc}$ (mg/g)	R^2	$K_2 \times 10^{-2}$ ((g/mg)/min)	$q_{e\ calc}$ (mg/g)	R^2
5	1.00	2.09	1.20	0.940	1.38	1.23	0.992
10	1.35	1.58	1.56	0.966	0.70	1.70	0.983
20	1.60	1.44	1.75	0.972	0.59	1.90	0.981
30	1.90	1.35	1.87	0.987	0.58	2.10	0.989
40	2.20	2.15	2.83	0.901	0.74	2.50	0.994

Table 2
Intra-particle diffusion parameters for the adsorption of PS nanoplastics at different initial concentrations by 5 g/L GAC in ultrapure water at 7.4 ± 0.1.

Ci (mg/L)	k_{d1} ((mg/g)/min$^{1/2}$)	C_1 (mg/g)	R^2	k_{d2} ((mg/g)/min$^{1/2}$)	C_2 (mg/g)	R^2
5	0.079	0.006	0.997	0.010	0.851	0.651
10	0.097	−0.024	0.998	0.033	0.835	0.945
20	0.111	−0.012	0.996	0.056	0.727	0.981
30	0.134	0.009	0.999	0.073	0.749	0.988
40	0.150	0.134	0.998	0.054	1.291	0.932

surface of the GAC through external mass transfer at faster rate than intra-particle diffusion. Once the external surface is saturated, PS nanoplastics diffuse into internal pores and are adsorbed within the internal surface of GAC.

3.2.4. Equilibrium adsorption studies

Equilibrium adsorption isotherms provide useful information about the adsorption process, adsorbent affinity and adsorption capacity (Ho et al., 2000). The most commonly used models, the Langmuir and Freundlich isotherms are both employed here. Langmuir isotherm assumes a monolayer adsorption onto solid surfaces, meaning that once an adsorption site is occupied, no further adsorption can take place at that site (Hameed, 2008; Langmuir, 1918). The Langmuir equation is expressed as follows:

$$\frac{C_e}{q_e} = \frac{1}{Q\ K_L} + \frac{C_e}{Q} \tag{7}$$

where q_e is the adsorption capacity at equilibrium (mg/g) and C_e is the PS concentration at equilibrium (mg/L). Q represents the maximum monolayer adsorption capacity (mg/g), and K_L the Langmuir constant (L/mg) determined from the slope and intercept of the linear plot of C_e/q_e as a function of C_e (Fig. S6a). The essential characteristics of the Langmuir isotherm can be expressed by a separation factor or equilibrium parameter (R_L) that is defined by the following equation (Shen et al., 2009).

$$R_L = \frac{1}{1 + K_L\ C_i} \tag{8}$$

where C_i is the PS nanoplastics initial concentration. The R_L value indicates if the nature of the adsorption process is unfavorable ($R_L > 1$), linear ($R_L = 1$), favorable ($0 < R_L < 1$) or irreversible ($R_L = 0$).

Freundlich isotherm is related to an empirical equation presuming that the adsorption process takes place on heterogeneous surfaces (Fu et al., 2015; Ijagbemi et al., 2009; Shukla et al., 2002). The linear expressions of the Freundlich equation is expressed as follows:

$$\log\ q_e = \log\ k_f + \frac{1}{n}\ \log\ C_e \tag{9}$$

The Freundlich constants k_f ((mg/g) (L/mg)$^{1/n}$) and 1/n are the adsorption capacity and the adsorption intensity, obtained from the intercept and slope of the plot log q_e versus log C_e (Fig. S6b). The magnitude of 1/n gives an indication of the favorability of adsorption and values of 1/n < 1 correspond to favorable adsorption (Saleh, 2015).

The results obtained for the Langmuir and Freundlich isotherms models are presented in Fig. S6 and Table S5. From the results, the correlation coefficient (R^2) value of the Langmuir model is found higher than the one calculated for the Freundlich model, 0.983 and 0.932 respectively (Table S5). Therefore, Langmuir isotherm seems to better describe the PS nanoplastics adsorption onto GAC indicating a monolayer adsorption reaction. Furthermore, the calculated monolayer adsorption capacity is found here to be 2.15 ± 0.05 mg/g which is close to the experimental value (2.20 ± 0.06 mg/g).

In our study, the obtained R_L values are in the range of 0.266 to 0.043, suggesting favorable adsorption of PS nanoplastics onto GAC in ultrapure water at pH 7.4 ± 0.1. It is also observed that the R_L value decreases with increasing PS concentration from 5 to 40 mg/L (Table S4). Results are supported by the parameter n in Freundlich isotherm found here to be equal to 8.08, suggesting favorable adsorption.

3.3. Batch adsorption studies in surface water

3.3.1. Effect of initial PS nanoplastics concentration and contact time

To get an insight into the effect of complex environmental conditions (pH, ionic composition, presence of natural organic matter) on PS nanoplastic adsorption process, natural surface water from Lake Geneva, used as drinking water resources, is considered in this section.

The adsorption capacity and GAC removal efficiency with increasing initial concentration of nanoplastics is shown in Fig. 4. Experiments were carried out in Lake Geneva water at pH 8.4 ± 0.1 and fixed GAC concentration of 5 g/L and rising PS nanoplastic concentration from 5 to 40 mg/L. Results indicate an increase of the adsorption capacity (mg/g) with increasing PS concentration and contact time. The removal efficiency of nanoplastics, which is given in Fig. 4b, increases from 78% to 90% with increasing concentration from 5 mg/L to 20 mg/L, then a slight decrease is observed with increasing concentration.

The adsorption capacity and removal of PS nanoplastics in Lake Geneva water are generally higher than the values observed in ultrapure water (excepted for 5 mg/L PS) with a maximum experimental

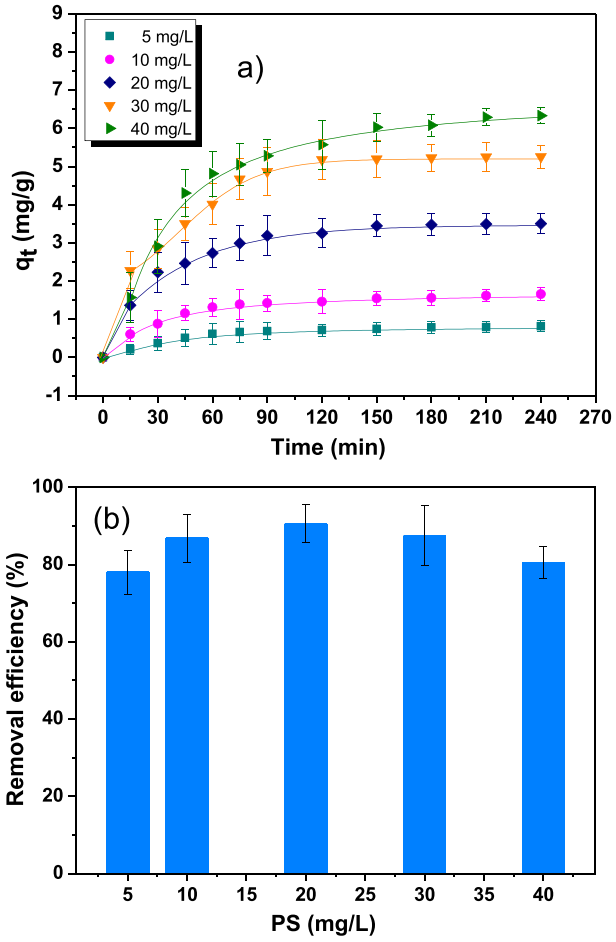

Fig. 4. (a) Effect of initial PS nanoplastics concentration and contact time on the adsorption capacity of 5 g/L GAC in Lake Geneva water at its natural pH (8.4 ± 0.1). (b) Effect of initial PS nanoplastics concentration on the removal efficiency at 5 g/L GAC in Lake Geneva water at its natural pH after 240 min of contact. Experiments were carried out at room temperature and shaker agitation speed of 100 rpm.

adsorption capacity equal to 6.33 ± 0.20 mg/g, compared to 2.20 ± 0.06 mg/g for ultrapure water. This improvement in the adsorption is partly due to the decrease of ζ-potential that leads to the destabilization and aggregation of PS nanoplastics (Fig. 5a).

In surface waters, NOM can significantly modify the stability of NPs promoting aggregation (or disaggregation) at higher NOM concentrations as reported by Loosli et al. (2014). As shown in Fig. 5, in Lake Geneva, the presence of 0.80 ± 0.05 mg/L of DOC (Table S2), is influencing the PS nanoplastics surface charge and hydrodynamic diameters via the formation of aggregates. At lower PS concentration (5 and 10 mg/L) the Dissolved Organic Matter (DOM) coating is more significant, leading to charge inversion and the formation of PS nanoplastics-DOM complexes negatively charged. At higher PS concentrations (20, 30, and 40 mg/L), DOM adsorption effect is less significant and nanoplastics are again positively charged resulting in more favorable interactions between the negative GAC and the positive PS nanoplastics consequently increasing the adsorption capacity.

3.3.2. Equilibrium adsorption studies and kinetic adsorption rates

To investigate the adsorption behavior and rate-controlling steps during the adsorption of PS nanoplastics onto the GAC in natural surface waters, kinetic models and equilibrium isotherms were also applied to fit the experimental data.

The results obtained for the pseudo-first-order and pseudo-second-order kinetic model are presented in Fig. 6 and Table 3. They indicate that the pseudo-second-order kinetic model fits better the experimental

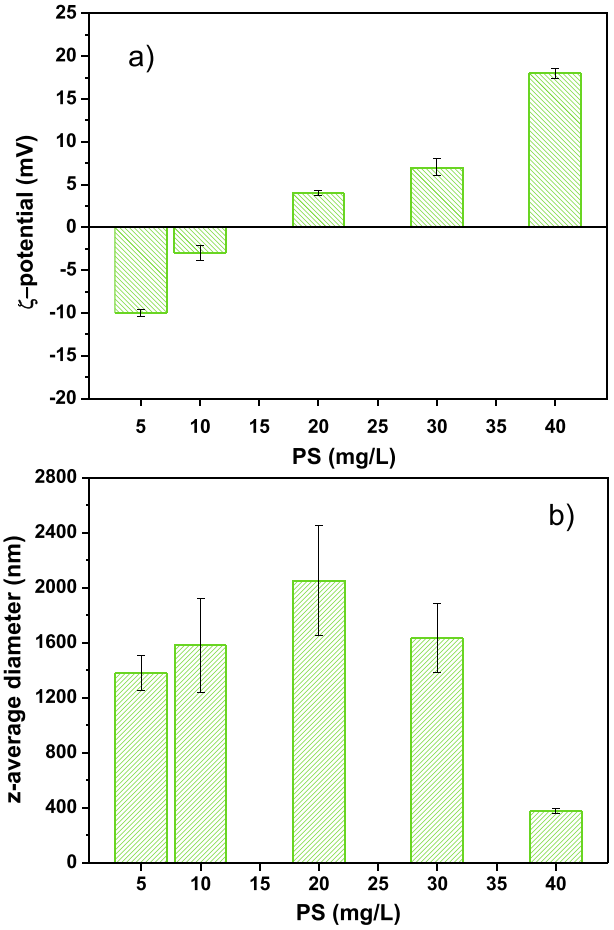

Fig. 5. (a) ζ-Potential and (b) z-average hydrodynamic diameter of PS nanoplastics at different initial concentrations in Lake Geneva water at its natural pH (8.4 ± 0.1) after 15 min of contact with 5 g/L GAC. PS nanoplastics are found negatively charged and to aggregate at low concentrations (5, 10 mg/L), positively charged and to aggregate at intermediate concentrations (20, 30 mg/L) and significantly positively charged and stable regarding aggregation at 40 mg/L.

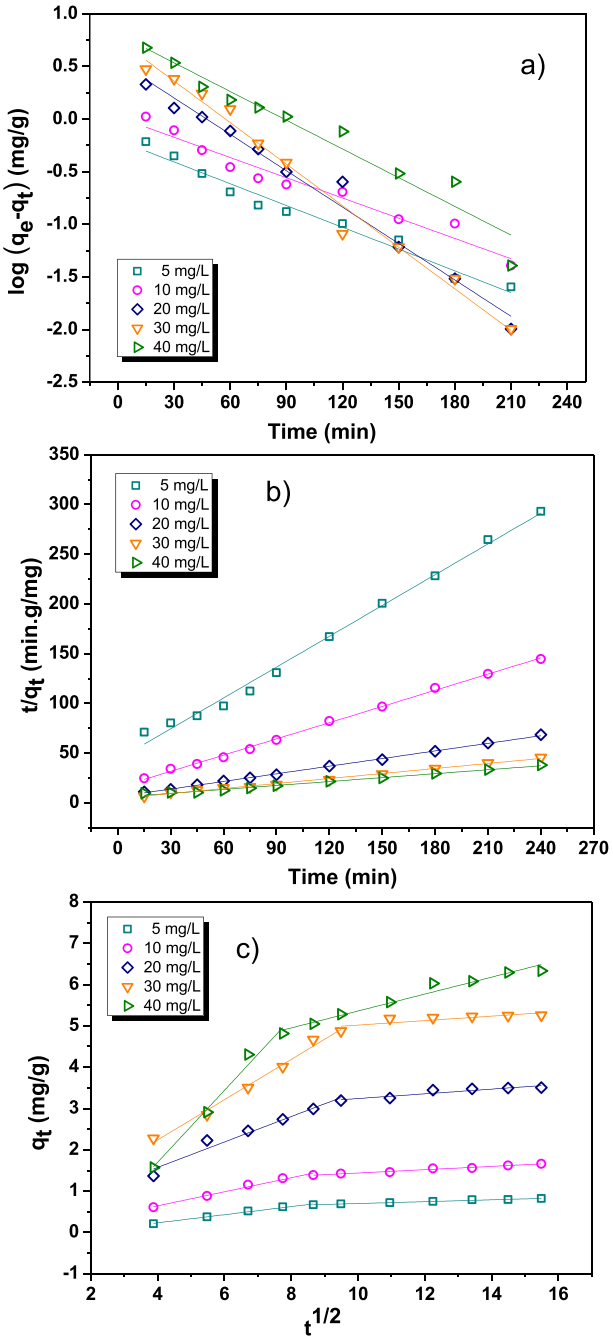

Fig. 6. (a) Pseudo-first order, (b) pseudo-second order and (c) intra-particle diffusion kinetic models for the adsorption of PS nanoplastics at different initial concentrations by GAC in Lake Geneva water at its natural pH (8.4 ± 0.1). The pseudo-second order kinetic model fit better the experimental data with a correlation coefficient of 0.98.

data than the pseudo-first-order model. The calculated adsorption capacity $q_{e,cal}$ values are close to the experimental values with correlation coefficient values greater than 0.99 for all PS initial concentrations. This indicates that the rate of PS nanoplastics adsorption by GAC in Lake Geneva water is also expected to be controlled by chemisorption. As shown for ultrapure water, the rate constant value k_2 increases with decreasing PS nanoparticles initial concentration indicating a faster adsorption at lower PS concentration. It is found that k_2 values are higher in Lake Geneva water than in ultrapure water, excepted at 40 mg/L PS nanoplastics, suggesting that aggregation and PS nanoplastic surface charge have an important effect on the adsorption kinetic results of PS nanoplastics.

Table 3
Pseudo-first-order and pseudo-second-order kinetic parameters for the adsorption of PS nanoplastics at different initial concentrations by 5 g/L GAC in Lake Geneva water at its natural pH (8.4 ± 0.1). Experimental conditions: room temperature, contact time of 240 min and shaker agitation speed of 100 rpm.

C_i (mg/L)	$q_{e\ exp}$ (mg/g)	Pseudo-first-order			Pseudo-second-order		
		$K_1 \times 10^{-2}$ (1/min)	$q_{e\ calc}$ (mg/g)	R^2	$K_2 \times 10^{-2}$ ((g/mg)/min)	$q_{e\ calc}$ (mg/g)	R^2
5	0.82	1.64	0.46	0.977	3.43	0.95	0.994
10	1.66	1.56	1.18	0.960	2.35	1.83	0.998
20	3.50	2.65	3.52	0.986	1.31	3.70	0.999
30	5.25	3.02	5.60	0.986	0.84	5.80	0.995
40	6.33	2.09	6.40	0.946	0.44	7.46	0.992

The intra-particle diffusion model is also applied in Lake Geneva Water to investigate PS nanoplastics diffusion mechanism to and into GAC. As shown in Fig. 6c, the plot of q_t versus $t^{1/2}$ shows two distinct regions. The first region of the plot is attributed to external mass transfer, while the second region is attributed to intra-particle diffusion process, indicating that intra-particle diffusion is not the only rate-controlling step in the adsorption process of PS nanoplastics by the GAC. The values of the rate constants obtained from the two linear portions and the correlations coefficients (R^2) are presented in Table 4. Rate constants indicate that PS nanoplastics as individuals or aggregates are transported to the surface of the GAC through external mass transfer at faster rate than intra-particle diffusion.

Rate constants k_{d1} obtained for PS nanoplastics in Lake Geneva water are found higher than those for ultrapure water due to the effect of aggregation and sedimentation whereas k_{d2} indicate that internal diffusion is less efficient in Lake Geneva water.

The Langmuir and Freundlich isotherms models and the corresponding correlation coefficient (R^2) values are given in Fig. S8 and Table S6. From the results, neither Langmuir nor Freundlich models are describing in a satisfactory way the adsorption of PS nanoplastics onto the activated carbon. Indeed, the R^2 value of the Langmuir model is much lower than 1 and the R^2 of Freundlich model despite higher (0.82), remains still low.

3.4. Adsorption mechanisms of PS nanoplastics by activated carbon in ultrapure and surface waters

Our results indicate that to get an insight into adsorption mechanisms it is first important to understand PS transformations and interactions with water constituents. Schematic representations of possible mechanisms of PS nanoplastic adsorption by GAC in ultrapure and surface waters are given in Figs. 7 and 8 and illustrated with SEM images.

In ultrapure water, PS nanoplastics are positively charged and stable during the experimental time and no variations in the PS hydrodynamic diameter are observed (Fig. 7a). Consequently, and as shown by SEM (Fig. 7b), nanoplastic particles are adsorbed onto the GAC surface as well as into the comparatively large pores mainly as individuals. In addition, as expected from the adsorption isotherms, nanoplastics are well adsorbed as a homogeneous monolayer. In Fig. 7c, a schematic representation of the adsorption-diffusion mechanism is presented.

Table 4
Intra-particle diffusion parameters for the adsorption of PS nanoplastics at different initial concentrations by 5 g/L GAC in Lake Geneva water at its natural pH (8.4 ± 0.1).

C_i (mg/L)	k_{d1} ((mg/g)/min$^{1/2}$)	C_1 (mg/g)	R^2	k_{d2} ((mg/g)/min$^{1/2}$)	C_2 (mg/g)	R^2
5	0.098	−0.162	0.992	0.022	0.473	0.988
10	0.170	−0.036	0.990	0.040	1.038	0.983
20	0.308	0.342	0.964	0.057	2.672	0,872
30	0.487	0.290	0.989	0.054	4.478	0.692
40	0.871	−1.782	0.986	0.205	3.311	0.968

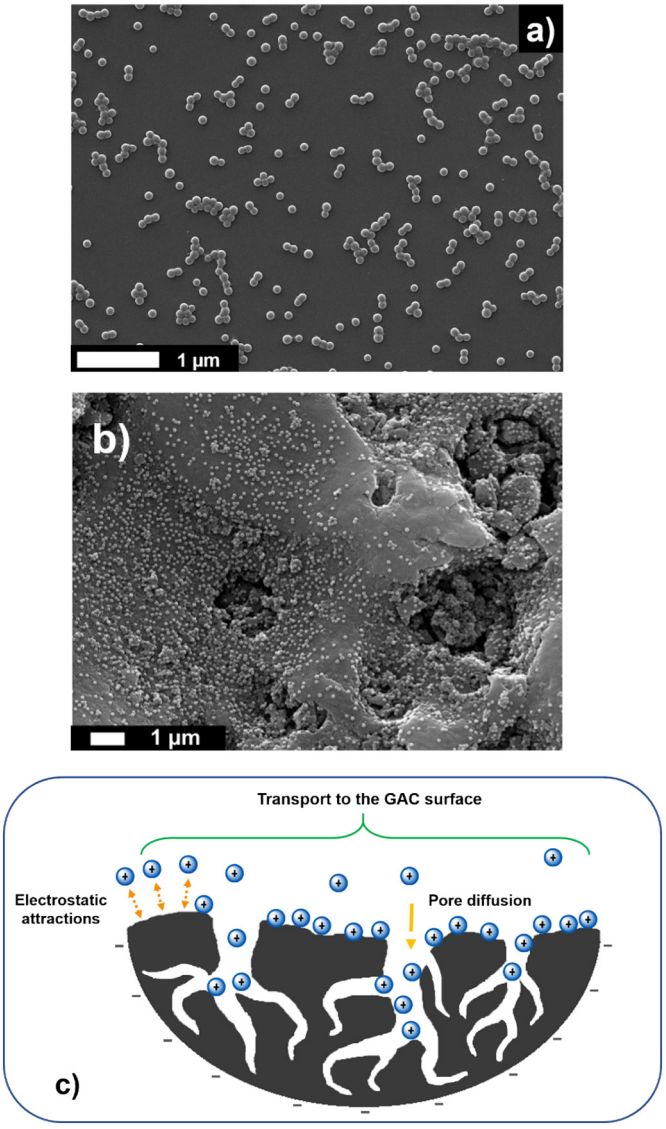

Fig. 7. (a) SEM image of PS nanoplastics in ultrapure water at pH 7.4 ± 0.1; [PS] = 5 mg/L. (b) SEM image of PS nanoplastics adsorbed onto GAC in ultrapure water at pH 7.4 ± 0.1: [PS] = 20 mg/L. Nanoplastic are principally adsorbed as individual particles onto the GAC surface and into the pores. (c) Proposed mechanism of PS nanoplastic adsorption and removal by GAC in ultrapure water. Adsorption and removal of nanoplastics are mainly due to electrostatic interactions between the positively charged nanoplastics and negatively charged GAC.

Nanoplastic particles are transported from the suspension towards the external activated carbon surface and then migrate into the pores. As PS nanoplastics are strongly positively charged in ultrapure water at pH 7.4 ± 0.1, their adsorption by the negatively charged activated carbon is dominated by electrostatic attractions which explain the formation of a homogeneous monolayer.

In Lake Geneva water the presence of DOM and divalent cations is strongly influencing the surface charge and hydrodynamic diameter via the formation of aggregates (Fig. 5). These results are supported by SEM images (Fig. 8a), where nanoplastics form large aggregates and are found embedded into a complex organic matter matrix. The electrostatic attraction between negatively charged DOM and positively charged nanoplastics leads to the adsorption of DOM onto PS surface which can modify their stability via surface charge neutralization as observed by Yu et al. (2019) and Oriekhova and Stoll (2018). Divalent ions are also expected to interact with PS nanoplastics and negatively charged NOM, forming bridges between them and promote their

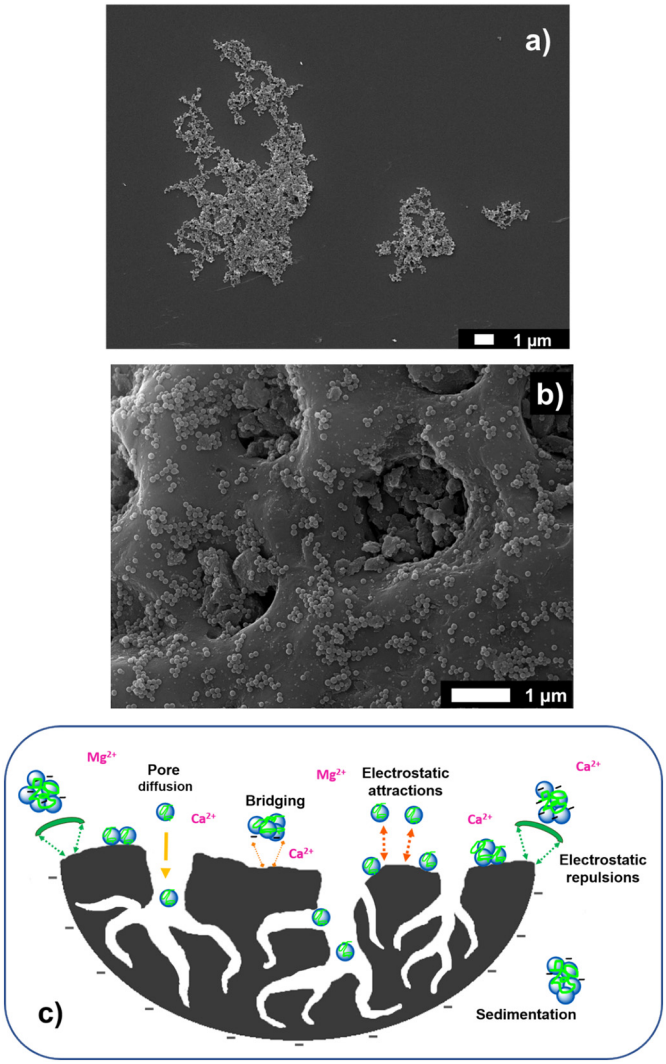

Fig. 8. (a) SEM image of PS nanoplastics in Lake Geneva water; [PS] = 20 mg/L. Nanoplastics are found aggregated and embedded in an organic matter matrix. (b) SEM image of PS nanoplastics adsorbed onto GAC in Lake Geneva water; [PS] = 20 mg/L. PS nanoplastics are adsorbed onto the GAC surface mainly as aggregates, some individual particles and poor migration into the pores is observed compared to ultrapure water. (c) Schematic representation of proposed mechanism of PS nanoplastic adsorption and removal by GAC in surface. Adsorption and removal of positively charged nanoplastics are governed by the presence of DOM.

aggregation (Buffle et al., 1998). SEM results, presented in Fig. 8b, indicate that nanoplastics are mainly adsorbed as aggregates and poor migration into the pores is observed in agreement with the intra-particle diffusion model.

A schematic representation of PS nanoplastics adsorption mechanism in Lake Geneva water is presented in Fig. 8c. As illustrated, PS nanoplastics can be found in solution as aggregates and individual particles coated with DOM and are principally adsorbed as aggregates onto the GAC surface. It is also found that nanoplastics diffusion into the GAC pores is less efficient because of the formation of large aggregates. Compared to ultrapure water, the conditions in Lake Geneva water are less favorable to nanoplastics adsorption due to unfavorable electrostatic interactions between nanoplastics coated with negatively charged DOM and the negatively charged GAC surface. However, the presence of divalent cations such as Ca^{2+} and Mg^{2+} is expected to make possible adsorption on GAC creating new adsorption sites via bridging effects, in particular when DOM is forming negatively charged complexes with PS nanoplastics (Daifullah et al., 2004; Mazet et al., 1988), thus indicating that the PS nanoplastics and DOM ratio is also playing a role in the adsorption mechanisms.

4. Conclusions

In this work, adsorption capacity and removal efficiency of PS nanoplastics by granular activated carbon as well as the effect of complex environmental conditions on PS nanoplastic behavior and GAC adsorption process were investigated.

It was found that in ultrapure water the adsorption and removal of nanoplastics was dominated by electrostatic attractions between the positively charged PS nanoplastics and negatively charged GAC. Moreover, PS nanoplastic adsorption capacity was found to increase with increasing initial nanoplastic concentration with a maximum adsorption capacity equal to 2.20 ± 0.06 mg/g, while the removal efficiency decreased from 98% to 26%. Equilibrium studies were in good agreement with the Langmuir isotherm ($R^2 = 0.98$), indicating that the PS nanoplastics adsorption can be described by a monolayer adsorption reaction. The experimental data were found in good agreement with the pseudo-second-order model ($R^2 > 0.98$), therefore indicating the rate of PS nanoplastics adsorption controlled by chemisorption.

We also found that in natural surface water from Lake Geneva the adsorption process was significantly influenced by aggregation, indirectly promoting the adsorption capacity and removal of PS nanoplastics. Adsorption capacity was found to significantly increase with increasing PS nanoplastics concentration with a maximum adsorption capacity of 6.33 ± 0.20 mg/g. Higher removal efficiency was also observed in Lake Geneva water especially at higher nanoplastic concentrations (from 10 to 40 mg/L), reaching 90% of removal at 20 mg/L. The kinetic pseudo-second-order and intra-particle diffusion provided a good correlation with the experimental data ($R^2 > 0.99$). Results showed that the intra-particle diffusion was not the only rate-controlling step and that the external mass transfer process onto GAC surface was more important than for ultrapure water. On the other hand, neither Langmuir nor Freundlich models were describing in a satisfactory way the adsorption of PS nanoplastics by GAC due to the interplay between adsorption and aggregation.

Regarding the nanoplastics removal in conventional drinking water treatment plants, this study indicates that GAC produced from renewable sources can be considered as a moderate adsorbent for the removal of positively charged PS nanoplastics.

CRediT authorship contribution statement

Lina Ramirez Arenas: Conceptualization, Methodology, Software, Validation, Formal analysis, Investigation, Writing – original draft, Writing – review & editing, Visualization. **Stéphan Ramseier Gentile:** Resources, Writing – review & editing, Funding acquisition. **Stéphane Zimmermann:** Resources, Writing – review & editing, Funding acquisition. **Serge Stoll:** Conceptualization, Validation, Resources, Writing – review & editing, Supervision, Project administration, Funding acquisition.

Declaration of competing interest

The authors declare that they have no known competing financial interests or personal relationships that could have appeared to influence the work reported in this paper.

Acknowledgements

The authors acknowledge support received from FOWA (Grant 017-16) from Société Suisse de l'Industrie du Gaz et des Eaux SSIGE/SVGW, Service Industriel de Genève (SIG) and University of Geneva. We are also grateful to Agathe Martignier for her support during the SEM measurements.

Appendix A. Supplementary data

Supplementary data to this article can be found online at https://doi.org/10.1016/j.scitotenv.2021.148175.

References

Alimi, O.S., Farner Budarz, J., Hernandez, L.M., Tufenkji, N., 2018. Microplastics and nanoplastics in aquatic environments: aggregation, deposition, and enhanced contaminant transport. Environ. Sci. Technol. 52 (4), 1704–1724.

Baalousha, M., 2009. Aggregation and disaggregation of iron oxide nanoparticles: influence of particle concentration, pH and natural organic matter. Sci. Total Environ. 407 (6), 2093–2101.

Baalousha, M., Le Coustumer, P., Jones, I., Lead, J.R., 2010. Characterisation of structural and surface speciation of representative commercially available cerium oxide nanoparticles. Environ. Chem. 7 (4), 377–385.

Bergami, E., Pugnalini, S., Vannuccini, M.L., Manfra, L., Faleri, C., Savorelli, F., Dawson, K.A., Corsi, I., 2017. Long-term toxicity of surface-charged polystyrene nanoplastics to marine planktonic species Dunaliella tertiolecta and Artemia franciscana. Aquat. Toxicol. 189, 159–169.

Besseling, E., Quik, J.T.K., Sun, M., Koelmans, A.A., 2017. Fate of nano- and microplastic in freshwater systems: a modeling study. Environ. Pollut. 220, 540–548.

Bhatt, I., Tripathi, B.N., 2011. Interaction of engineered nanoparticles with various components of the environment and possible strategies for their risk assessment. Chemosphere 82 (3), 308–317.

Bhattacharyya, K.G., Gupta, S.S., 2008. Kaolinite and montmorillonite as adsorbents for Fe (III), Co(II) and Ni(II) in aqueous medium. Appl. Clay Sci. 41 (1), 1–9.

Buffle, J., Wilkinson, K.J., Stoll, S., Filella, M., Zhang, J., 1998. A generalized description of aquatic colloidal interactions: the three-colloidal component approach. Environ. Sci. Technol. 32 (19), 2887–2899.

Chowdhury, I., Hong, Y., Honda, R.J., Walker, S.L., 2011. Mechanisms of TiO_2 nanoparticle transport in porous media: role of solution chemistry, nanoparticle concentration, and flowrate. J. Colloid Interface Sci. 360 (2), 548–555.

Daifullah, A.A.M., Girgis, B.S., Gad, H.M.H., 2004. A study of the factors affecting the removal of humic acid by activated carbon prepared from biomass material. Colloids Surf. A Physicochem. Eng. Asp. 235 (1), 1–10.

Degenkolb, L., Metreveli, G., Philippe, A., Brandt, A., Leopold, K., Zehlike, L., Vogel, H.-J., Schaumann, G.E., Baumann, T., Kaupenjohann, M., Lang, F., Kumahor, S., Klitzke, S., 2018. Retention and remobilization mechanisms of environmentally aged silver nanoparticles in an artificial riverbank filtration system. Sci. Total Environ. 645, 192–204.

Dong, S., Cai, W., Xia, J., Sheng, L., Wang, W., Liu, H., 2021. Aggregation kinetics of fragmental PET nanoplastics in aqueous environment: complex roles of electrolytes, pH and humic acid. Environ. Pollut. 268, 115828.

Ebrahimian Pirbazari, A., Saberikhah, E., Badrouh, M., Emami, M.S., 2014. Alkali treated Foumanat tea waste as an efficient adsorbent for methylene blue adsorption from aqueous solution. Water Resour. Ind. 6, 64–80.

Eerkes-Medrano, D., Thompson, R.C., Aldridge, D.C., 2015. Microplastics in freshwater systems: a review of the emerging threats, identification of knowledge gaps and prioritisation of research needs. Water Res. 75, 63–82.

Ekmekyapar, F., Aslan, A., Bayhan, Y.K., Cakici, A., 2006. Biosorption of copper(II) by nonliving lichen biomass of Cladonia rangiformis hoffm. J. Hazard. Mater. 137 (1), 293–298.

Enfrin, M., Dumée, L.F., Lee, J., 2019. Nano/microplastics in water and wastewater treatment processes — origin, impact and potential solutions. Water Res. 161, 621–638.

Foo, K.Y., Hameed, B.H., 2009. An overview of landfill leachate treatment via activated carbon adsorption process. J. Hazard. Mater. 171 (1), 54–60.

Fu, J., Chen, Z., Wang, M., Liu, S., Zhang, J., Zhang, J., Han, R., Xu, Q., 2015. Adsorption of methylene blue by a high-efficiency adsorbent (polydopamine microspheres): kinetics, isotherm, thermodynamics and mechanism analysis. Chem. Eng. J. 259, 53–61.

Gigault, J., Pedrono, B., Maxit, B., Ter Halle, A., 2016. Marine plastic litter: the unanalyzed nano-fraction. Environ. Sci. Nano 3 (2), 346–350. https://doi.org/10.1039/C6EN00008H.

Gregory, J., 1998. Turbidity and beyond. Filtr. Separ. 35 (1), 63–67.

Hameed, B.H., 2008. Equilibrium and kinetic studies of methyl violet sorption by agricultural waste. J. Hazard. Mater. 154 (1), 204–212.

Hernandez, L.M., Yousefi, N., Tufenkji, N., 2017. Are there nanoplastics in your personal care products? Environ. Sci. Technol. Lett. 4 (7), 280–285.

Ho, Y.S., McKay, G., 1999. Pseudo-second order model for sorption processes. Process Biochem. 34 (5), 451–465.

Ho, Y.S., Ng, J.C.Y., McKay, G., 2000. Kinetics of pollutant sorption by biosorbents: review. Separ. Purif. Methods 29 (2), 189–232.

Ijagbemi, C.O., Baek, M.-H., Kim, D.-S., 2009. Montmorillonite surface properties and sorption characteristics for heavy metal removal from aqueous solutions. J. Hazard. Mater. 166 (1), 538–546.

Inyang, M., Gao, B., Wu, L., Yao, Y., Zhang, M., Liu, L., 2013. Filtration of engineered nanoparticles in carbon-based fixed bed columns. Chem. Eng. J. 220, 221–227.

Kamrani, S., Rezaei, M., Kord, M., Baalousha, M., 2018. Transport and retention of carbon dots (CDs) in saturated and unsaturated porous media: role of ionic strength, pH, and collector grain size. Water Res. 133, 338–347.

Labille, J., Harns, C., Bottero, J.-Y., Brant, J., 2015. Heteroaggregation of titanium dioxide nanoparticles with natural clay colloids. Environ. Sci. Technol. 49 (11), 6608–6616.

Lambert, S., Wagner, M., 2016. Characterisation of nanoplastics during the degradation of polystyrene. Chemosphere 145, 265–268.

Langmuir, I., 1918. The adsorption of gases on plane surfaces of glass, mica and platinum. J. Am. Chem. Soc. 40 (9), 1361–1403.

Largitte, L., Pasquier, R., 2016. A review of the kinetics adsorption models and their application to the adsorption of lead by an activated carbon. Chem. Eng. Res. Des. 109, 495–504.

Li, Z., Aly Hassan, A., Sahle-Demessie, E., Sorial, G.A., 2013. Transport of nanoparticles with dispersant through biofilm coated drinking water sand filters. Water Res. 47 (17), 6457–6466.

Liu, J., Ma, Y., Zhu, D., Xia, T., Qi, Y., Yao, Y., Guo, X., Ji, R., Chen, W., 2018. Polystyrene nanoplastics-enhanced contaminant transport: role of irreversible adsorption in glassy polymeric domain. Environ. Sci. Technol. 52 (5), 2677–2685.

Loosli, F., Le Coustumer, P., Stoll, S., 2014. Effect of natural organic matter on the disagglomeration of manufactured TiO_2 nanoparticles. Environ. Sci. Nano 1 (2), 154–160. https://doi.org/10.1039/C3EN00061C.

Lowry, G.V., Hill, R.J., Harper, S., Rawle, A.F., Hendren, C.O., Klaessig, F., Nobbmann, U., Sayre, P., Rumble, J., 2016. Guidance to improve the scientific value of zeta-potential measurements in nanoEHS. Environ. Sci. Nano 3 (5), 953–965. https://doi.org/10.1039/C6EN00136J.

Mattsson, K., Hansson, L.A., Cedervall, T., 2015. Nano-plastics in the aquatic environment. Environ Sci Process Impacts 17 (10), 1712–1721. https://doi.org/10.1039/C5EM00227C.

Mazet, M., Yaacoubi, A., Lafrance, P., 1988. Influence des ions metalliques liberes par un charbon actif sur l'adsorption de micropolluants organiques. Le role des ions calcium. Water Res. 22 (10), 1321–1329.

McGillicuddy, E., Morrison, L., Cormican, M., Dockery, P., Morris, D., 2018. Activated charcoal as a capture material for silver nanoparticles in environmental water samples. Sci. Total Environ. 645, 356–362.

Mintenig, S.M., Löder, M.G.J., Primpke, S., Gerdts, G., 2019. Low numbers of microplastics detected in drinking water from ground water sources. Sci. Total Environ. 648, 631–635.

Murphy, F., Ewins, C., Carbonnier, F., Quinn, B., 2016. Wastewater treatment works (WwTW) as a source of microplastics in the aquatic environment. Environ. Sci. Technol. 50 (11), 5800–5808.

Murray, A., Örmeci, B., 2020. Removal effectiveness of nanoplastics (<400 nm) with separation processes used for water and wastewater treatment. Water 12 (3), 635.

Mutemi, S., Hoko, Z., Makurira, H., 2020. Investigating feasibility of use of bio-sand filters for household water treatment in Epworth, Zimbabwe. Phys. Chem. Earth Pt A/B/C 117, 102864.

Novotna, K., Cermakova, L., Pivokonska, L., Cajthaml, T., Pivokonsky, M., 2019. Microplastics in drinking water treatment – current knowledge and research needs. Sci. Total Environ. 667, 730–740.

Okonji, S.O., Yu, L., Dominic, J.A., Pernitsky, D., Achari, G., 2021. Adsorption by granular activated carbon and nano zerovalent iron from wastewater: a study on removal of selenomethionine and selenocysteine. Water 13 (1), 23.

Oriekhova, O., Stoll, S., 2018. Heteroaggregation of nanoplastic particles in the presence of inorganic colloids and natural organic matter. Environ. Sci. Nano https://doi.org/10.1039/C7EN01119A.

Ortelli, S., Costa, A.L., Blosi, M., Brunelli, A., Badetti, E., Bonetto, A., Hristozov, D., Marcomini, A., 2017. Colloidal characterization of CuO nanoparticles in biological and environmental media. Environ. Sci. Nano 4 (6), 1264–1272. https://doi.org/10.1039/C6EN00601A.

Park, C.M., Chu, K.H., Her, N., Jang, M., Baalousha, M., Heo, J., Yoon, Y., 2017. Occurrence and removal of engineered nanoparticles in drinking water treatment and wastewater treatment processes. Separ. Purif. Rev. 46 (3), 255–272.

Piai, L., Blokland, M., van der Wal, A., Langenhoff, A., 2020. Biodegradation and adsorption of micropollutants by biological activated carbon from a drinking water production plant. J. Hazard. Mater. 388, 122028.

Piplai, T., Kumar, A., Alappat, B.J., 2017. Removal of mixture of ZnO and CuO nanoparticles (NPs) from water using activated carbon in batch kinetic studies. Water Sci. Technol. 75 (4), 928–943.

Pivokonsky, M., Cermakova, L., Novotna, K., Peer, P., Cajthaml, T., Janda, V., 2018. Occurrence of microplastics in raw and treated drinking water. Sci. Total Environ. 643, 1644–1651.

Praetorius, A., Badetti, E., Brunelli, A., Clavier, A., Gallego-Urrea, J.A., Gondikas, A., Hassellöv, M., Hofmann, T., Mackevica, A., Marcomini, A., Peijnenburg, W., Quik, J.T.K., Seijo, M., Stoll, S., Tepe, N., Walch, H., von der Kammer, F., 2020. Strategies for determining heteroaggregation attachment efficiencies of engineered nanoparticles in aquatic environments. Environ. Sci. Nano 7 (2), 351–367. https://doi.org/10.1039/C9EN01016E.

Ramirez, L., Ramseier Gentile, S., Zimmermann, S., Stoll, S., 2019. Behavior of TiO_2 and CeO_2 nanoparticles and polystyrene nanoplastics in bottled mineral, drinking and Lake Geneva waters. Impact of water hardness and natural organic matter on nanoparticle surface properties and aggregation. Water 11 (4).

Rengaraj, S., Yeon, K.-H., Kang, S.-Y., Lee, J.-U., Kim, K.-W., Moon, S.-H., 2002. Studies on adsorptive removal of Co(II), Cr(III) and Ni(II) by IRN77 cation-exchange resin. J. Hazard. Mater. 92 (2), 185–198.

Rochman, C.M., Kross, S.M., Armstrong, J.B., Bogan, M.T., Darling, E.S., Green, S.J., Smyth, A.R., Veríssimo, D., 2015. Scientific evidence supports a ban on microbeads. Environ. Sci. Technol. 49 (18), 10759–10761.

Rottman, J., Platt, L.C., Sierra-Alvarez, R., Shadman, F., 2013. Removal of TiO_2 nanoparticles by porous media: effect of filtration media and water chemistry. Chem. Eng. J. 217, 212–220.

Saavedra, J., Stoll, S., Slaveykova, V.I., 2019. Influence of nanoplastic surface charge on eco-corona formation, aggregation and toxicity to freshwater zooplankton. Environ. Pollut. 252, 715–722.

Saleh, T.A., 2015. Isotherm, kinetic, and thermodynamic studies on Hg(II) adsorption from aqueous solution by silica-multiwall carbon nanotubes. Environ. Sci. Pollut. Res. 22 (21), 16721–16731.
Saleh, T.A., 2020. Nanomaterials: classification, properties, and environmental toxicities. Environ. Technol. Innov. 20, 101067.
Shams, M., Alam, I., Chowdhury, I., 2020. Aggregation and stability of nanoscale plastics in aquatic environment. Water Res. 171, 115401.
Shen, D., Fan, J., Zhou, W., Gao, B., Yue, Q., Kang, Q., 2009. Adsorption kinetics and isotherm of anionic dyes onto organo-bentonite from single and multisolute systems. J. Hazard. Mater. 172 (1), 99–107.
Shukla, A., Zhang, Y.-H., Dubey, P., Margrave, J.L., Shukla, S.S., 2002. The role of sawdust in the removal of unwanted materials from water. J. Hazard. Mater. 95 (1), 137–152.
Sobhani, Z., Zhang, X., Gibson, C., Naidu, R., Megharaj, M., Fang, C., 2020. Identification and visualisation of microplastics/nanoplastics by Raman imaging (i): down to 100 nm. Water Res. 174, 115658.
Tian, L., Chen, Q., Jiang, W., Wang, L., Xie, H., Kalogerakis, N., Ma, Y., Ji, R., 2019. A carbon-14 radiotracer-based study on the phototransformation of polystyrene nanoplastics in water versus in air. Environ. Sci. Nano 6 (9), 2907–2917. https://doi.org/10.1039/C9EN00662A.
Tong, M., He, L., Rong, H., Li, M., Kim, H., 2020. Transport behaviors of plastic particles in saturated quartz sand without and with biochar/Fe_3O_4-biochar amendment. Water Res. 169, 115284.
Wang, W., Yuan, W., Chen, Y., Wang, J., 2018. Microplastics in surface waters of Dongting Lake and Hong Lake, China. Sci. Total Environ. 633, 539–545.
Weber, W.J., Morris, J.C., 1963. Kinetics of adsorption on carbon from solution. J. Sanit. Eng. Div. 89 (2), 31–60.
Wu, P., Cai, Z., Jin, H., Tang, Y., 2019. Adsorption mechanisms of five bisphenol analogues on PVC microplastics. Sci. Total Environ. 650, 671–678.
Xu, B., Zhai, Y., Zhu, Y., Peng, C., Wang, T., Zhang, C., Li, C., Zeng, G., 2016. The adsorption mechanisms of ClO_4^- onto highly graphited and hydrophobic porous carbonaceous materials from biomass. RSC Adv. 6 (96), 93975–93984. https://doi.org/10.1039/C6RA13341J.
Yu, S., Shen, M., Li, S., Fu, Y., Zhang, D., Liu, H., Liu, J., 2019. Aggregation kinetics of different surface-modified polystyrene nanoparticles in monovalent and divalent electrolytes. Environ. Pollut. 255, 113302.
Zhang, B., Chao, J., Chen, L., Liu, L., Yang, X., Wang, Q., 2021. Research progress of nanoplastics in freshwater. Sci. Total Environ. 757, 143791.
Zhang, H., Liu, F.-f, Wang, S.-c, Huang, T.-y, Li, M.-r, Zhu, Z.-l, Liu, G.-z, 2020a. Sorption of fluoroquinolones to nanoplastics as affected by surface functionalization and solution chemistry. Environ. Pollut. 262, 114347.
Zhang, Q., Xu, E.G., Li, J., Chen, Q., Ma, L., Zeng, E.Y., Shi, H., 2020b. A review of microplastics in table salt, drinking water, and air: direct human exposure. Environ. Sci. Technol. 54 (7), 3740–3751.
Zhang, Y., Diehl, A., Lewandowski, A., Gopalakrishnan, K., Baker, T., 2020c. Removal efficiency of micro- and nanoplastics (180 nm–125 μm) during drinking water treatment. Sci. Total Environ. 720, 137383.